Inorganic Chemistry

Article

pubs.acs.org/IC

Electrochemistry of Platinum(II) Porphyrins: Effect of Substituents and π-Extension on Redox Potentials and Site of Electron Transfer

Ping Chen,[†] Olga S. Finikova,[‡] Zhongping Ou,*[,†,§] Sergei A. Vinogradov,*[,‡] and Karl M. Kadish*[,†]

[†]Department of Chemistry, University of Houston, Houston, Texas 77204-5003, United States

[‡]Department of Biochemistry and Biophysics, University of Pennsylvania, Philadelphia, Pennsylvania 19104, United States

[§]Department of Applied Chemistry, Jiangsu University, Zhenjiang 212013, P. R. China

Supporting Information

ABSTRACT: Fourteen platinum(II) porphyrins with different π-conjugated macrocycles and different electron-donating or electron-withdrawing substituents were investigated as to their electrochemical and spectroscopic properties in nonaqueous media. Eight compounds have the formula $(Ar_4P)Pt^{II}$, where Ar_4P = the dianion of a tetraarylporphyrin, while six have π-extented macrocycles with four β,β′-fused benzo or naphtho groups and are represented as $(TBP)Pt^{II}$ and $(TNP)Pt^{II}$ where TBP and TNP are the dianions of tetrabenzoporphyrin and tetranaphthoporphyrin, respectively.

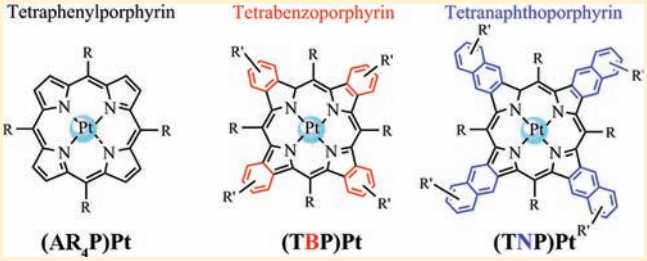

Each Pt(II) porphyrin undergoes two reversible one-electron reductions and one to three reversible one-electron oxidations in nonaqueous media. These reactions were characterized by cyclic voltammetry, UV−visible thin-layer spectroelectrochemistry and in some cases by ESR spectroscopy. The two reductions invariably occur at the conjugated π-ring system to yield relatively stable Pt(II) π-anion radicals and dianions. The first oxidation leads to a stable π-cation radical for each investigated porphyrin; but in the case of tetraarylporphyrins containing electron-withdrawing substituents, the product of the second oxidation may undergo an internal electron transfer to give a Pt(IV) porphyrin with an unoxidized macrocycle. The effects of macrocycle structure on UV−visible spectra, oxidation/reduction potentials, and site of electron transfer are discussed.

INTRODUCTION

Platinum(II) porphyrins possess unique optical characteristics[1,2] and have been widely studied for their possible applications in medicine and technology. For example, the highly emissive triplet states of Pt(II) porphyrins have been used extensively in sensing[3−11] and biological imaging[12−21] of oxygen as well as in the construction of organic light-emitting devices.[22−28] Our own interest in platinum porphyrins has focused in part on their applications[8,10,19−21] and in part on elucidating oxidation−reduction potentials while at the same time spectroscopically characterizing the products of each redox reaction in nonaqueous media.[29,30]

Recently, we reported the first evidence for the reversible electrochemical conversion between a Pt(II) and a Pt(IV)) porphyrin.[30] The investigated compound was $(TPP)Pt^{II}$, where TPP is the dianion of tetraphenylporphyrin. This study is extended in the present article to include Pt(II) tetraarylporphyrins with different electron-donationg or electron-withdrawing substituents as well as substituted tetrabenzoporphyrins and tetranaphthoporphyrins, which have symmetrically extended π−ring systems. Although it has been well-documented that substituents at the β-pyrrolic positions of a porphyrin macrocycle affect both redox potentials and the site of electron transfer,[31,32] a detailed electrochemical study under the same experimental conditions of multiple Pt(II) porphyrins, having significantly different macrocyclic structures, has not been reported.

In the present work, eight of the investigated compounds have the formula $(Ar_4P)Pt^{II}$, where Ar_4P is the dianion of a tetraarylporphyrin (Chart 1), while six have a π-extended macrocycle with four β,β′-fused benzo or naphtho groups and are represented as $(TBP)Pt^{II}$ and $(TNP)Pt^{II}$, where TBP and TNP are the dianions of tetrabenzoporphyrin and tetranaphthoporphyrin, respectively (Chart 2). The electron transfer reactions of each Pt(II) porphyrin were characterized by cyclic voltammetry, UV−visible thin-layer spectroelectrochemistry, and, in some cases, by ESR spectroscopy. The effects of substituents and macrocycle extension on UV−visible spectra, redox potentials, and site of electron transfer are discussed.

EXPERIMENTAL SECTION

Materials. $(TPP)Pt^{II}$ **5** was purchased from Frontier Scientific, Inc. and used as received. All other porphyrins (**1**−**4** and **6**−**14**) were synthesized as described previously (see refs 29, 33, and 34, and references therein). Dichloromethane (CH_2Cl_2, 99.8%) was purchased from EMD Chemicals Inc. and used as received. Benzonitrile (PhCN) was purchased from Sigma-Aldrich Co. and freshly distilled over P_2O_5 before use. Tetra-*n*-butylammonium perchlorate (TBAP) was

Received: February 14, 2012
Published: May 24, 2012

   dx.doi.org/10.1021/ic3003367 | *Inorg. Chem.* 2012, 51, 6200−6210

Chart 1. Structures of Substituted Tetraarylporphyrins $(Ar_4P)Pt^{II}$ (1–8)

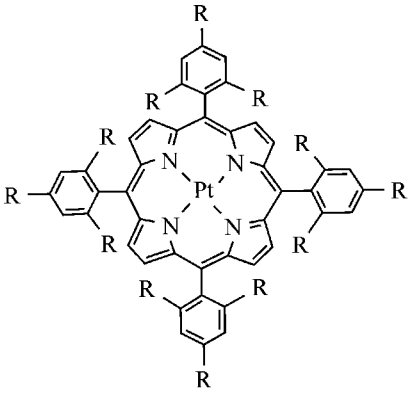

1. R = OMe

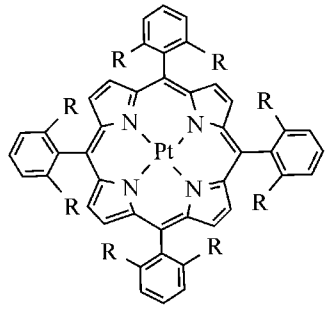

2. R = OMe

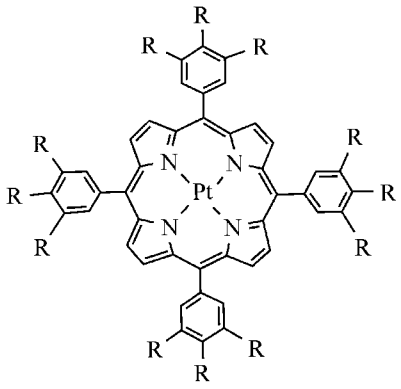

3. R = OMe

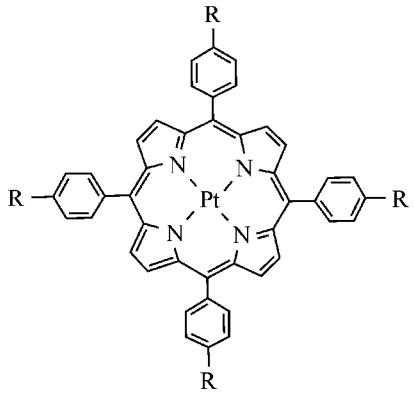

4. R = OCH_2CO_2Et
7. R = CO_2Me

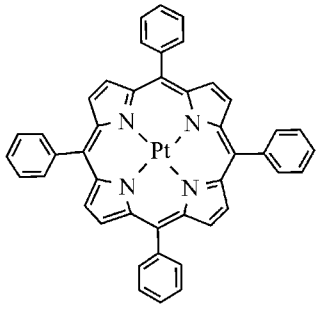

5. (TPP)Pt

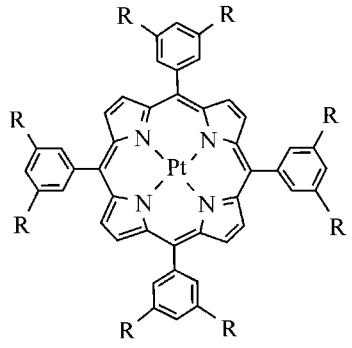

6. R = OMe
8. R = CO_2Bu

purchased from Sigma Chemical or Fluka Chemika Co., recrystallized from ethyl alcohol and dried under vacuum at 40 °C for at least one week prior to use.

Instrumentation. Cyclic voltammetry was carried out at 298 K using an EG&G Princeton Applied Research (PAR) 173 potentiostat/galvanostat. A homemade three-electrode cell was used for cyclic voltammetric measurements. It consisted of a glassy carbon working electrode, a platinum counter electrode, and a homemade saturated calomel reference electrode (SCE). The SCE was separated from the bulk solution by a fritted glass bridge of low porosity, which contained the solvent/supporting electrolyte mixture. An H-type cell with a fritted glass layer to separate the cathode and anode portions was used for bulk electrolysis. The working and counter electrodes were made from platinum mesh. Both the working and reference electrodes were placed in one compartment, while the counter electrode was in another compartment.

UV–visible spectra were measured using a Hewlett-Packard 8453 diode array spectrophotometer. Electron spin resonance (ESR) spectra were obtained on an IBM ESP 300 apparatus. Low temperature measurements were carried out using a liquid-nitrogen finger dewar. Thin-layer UV–visible spectroelectrochemical experiments were performed using a home-built thin-layer cell, which has a transparent platinum net working electrode. Potentials were applied and monitored with an EG&G PAR Model 173 potentiostat. High purity N_2 from Trigas was used to deoxygenate the solution. Solutions were kept under N_2 during each electrochemical and spectroelectrochemical experiment.

dx.doi.org/10.1021/ic3003367 | *Inorg. Chem.* 2012, 51, 6200–6210

Chart 2. Structures of Substituted Tetrabenzoporphyrins (TBP)Pt^{II} (9–12) and Tetranaphthylporphyrins (TNP)Pt^{II} (13 and 14)

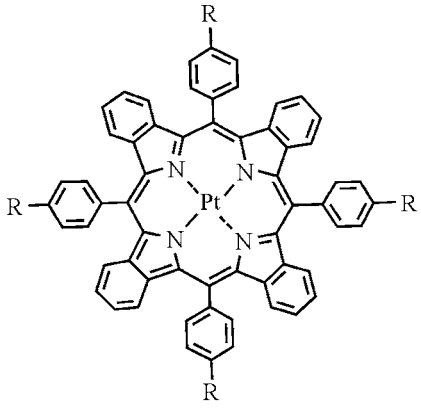

9. R = CO_2Me

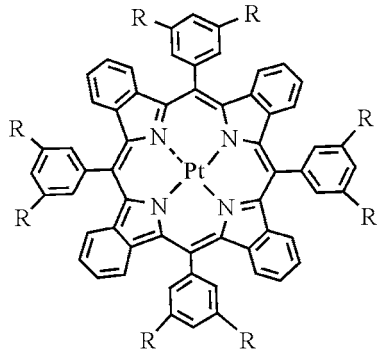

10. R = CO_2Bu

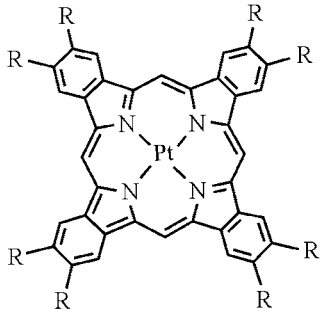

11. R = CO_2Bu

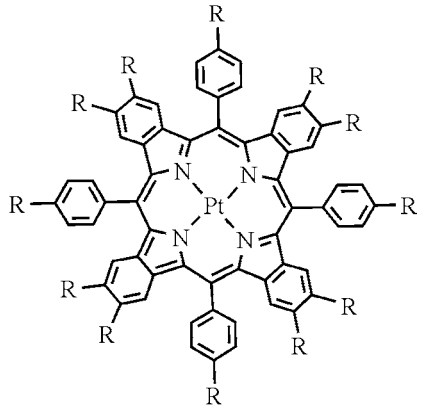

12. R = CO_2Me

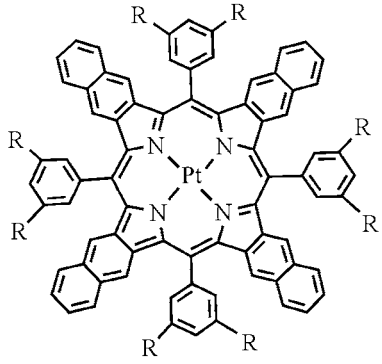

13. R = CO_2Bu

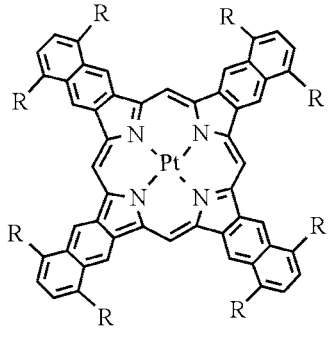

14. R = $O(CH_2)_3CO_2Bu$

RESULTS AND DISCUSSION

Electrochemistry of Pt(II) Tetraarylporphyrins. The redox properties of $(Ar_4P)Pt^{II}$ **1**–**8** were examined in CH_2Cl_2, PhCN, and DMF containing 0.2 M TBAP. Examples of cyclic voltammograms in CH_2Cl_2 are shown in Figure 1 for compounds **2**, **5**, and **7**, and the half-wave potentials for **1**–**8** in CH_2Cl_2 are summarized in Table 1.

Two reversible one-electron reductions are observed for **3**–**8**, while compounds **1** and **2**, which contain electron-donating substituents and therefore are harder to reduce, exhibit only one reduction above the solvent negative potential limit of −2.0 V vs SCE. The first reduction ranges from $E_{1/2}$ = −1.52 V for compound **1** to −1.14 V for compound **8** (see Table 1). The difference in half-wave potentials between the first and second reductions is listed in Table 1 as $\Delta red_{(1-2)}$ and ranges from 0.41 to 0.52 V, consistent with two stepwise porphyrin ring-centered one-electron transfer additions.[31] Almost no differences in $E_{1/2}$ are seen upon changing the solvent from CH_2Cl_2 (Table 1) to PhCN or DMF (Table S1), and this might be predicted based on the lack of solvent coordination to the central metal ion of

dx.doi.org/10.1021/ic3003367 | Inorg. Chem. 2012, 51, 6200–6210

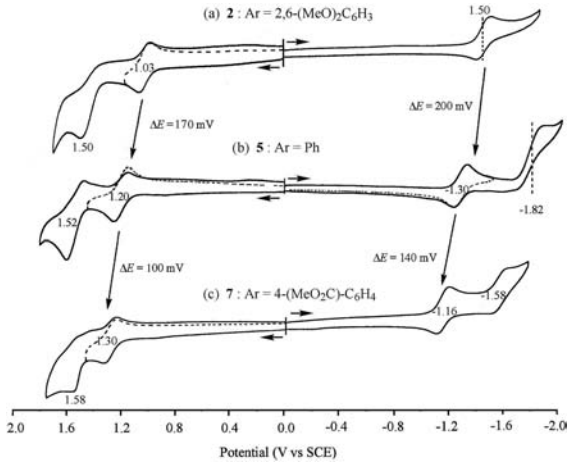

Figure 1. Cyclic voltammograms of $(Ar_4P)Pt^{II}$ **2**, **5**, and **7** in CH_2Cl_2, 0.2 M TBAP.

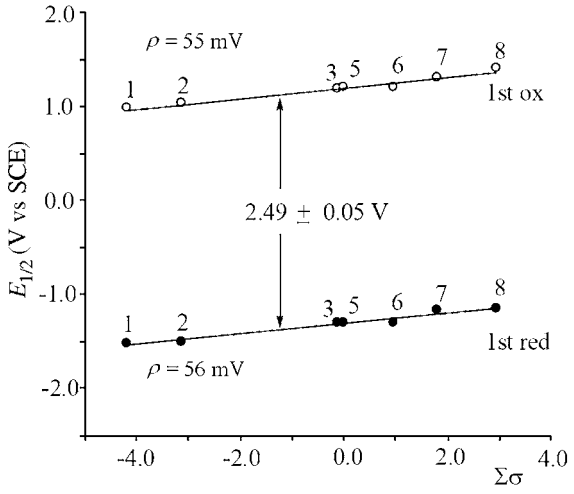

Figure 2. Plots of the half-wave potentials for the first reduction and first oxidation of $(Ar_4P)Pt^{II}$ in CH_2Cl_2 containing 0.1 M TBAP vs the Hammett substituent constants ($\Sigma\sigma$). Values of $E_{1/2}$ and $\Sigma\sigma$ are given in Table 1.

the reactant or product in the electron transfer reaction, i.e., the Pt(II) center remains four-coordinate in all three solvents.

The first oxidation of **1**−**8** is also reversible as expected for tetraarylporphyrins,[32] the measured $E_{1/2}$ values shifting positively or negatively with changes in the electron-donating/electron-withdrawing substituents at the four *meso*-position of the macrocycle. The relevant electrochemical linear free energy relationship is shown in Figure 2. The slope of the line in the plot is defined by the equation $\Delta E = \Sigma\sigma\rho$, where $\Sigma\sigma$ represents the sum of the substituent constants and ρ is the reaction constant.[35] The values of ρ for the first reduction and first oxidation of $(Ar_4P)Pt^{II}$ were calculated from the slope of the correlation in Figure 2 to be 56 and 55 mV, respectively. Similar ρ values, ca. 50−60 mV, have been reported for reduction and oxidation of related tetraarylporphyrins with different metal ions.[31,32,36]

The significance of the data in Figure 2 is 2-fold. First, all the compounds follow the same linear free energy relationship between $E_{1/2}$ and $\Sigma\sigma$, indicating the same electron transfer mechanism under the given set of experimental conditions. In addition, the slopes in Figure 2 (55−56 mV) are consistent with porphyrin ring-centered electron transfers,[31] and this is also the assignment based on the average electrochemical HOMO−LUMO gap of 2.49 ± 0.05 V for the eight compounds.

It has often been reported that the electrochemically measured HOMO−LUMO gap for tetraarylporphyrins is 2.25 ± 0.15 V, independent of the central metal ions.[32] This is generally true, but it should be pointed out that the separation in $E_{1/2}$ values between formation of porphyrin π-cation and π-anion radicals depends upon a number of variables, one of which is specific to the nature of the central metal ion. For example, the measured HOMO−LUMO gap of $(TPP)Pt^{II}$ is 2.50 V (see Table 1), which compares to 2.44 V for $(TPP)Pd^{II}$, 2.30 V for $(TPP)Ni^{II}$, 2.27 V for $(TPP)Cu^{II}$, and 2.15 V for $(TPP)Zn^{II}$ under the same conditions.[37] Whatever the HOMO−LUMO gap, a linear relationship between $E_{1/2}$ and $\Sigma\sigma$ indicates that the same electron transfer mechanism occurs for all compounds in the series[35,36] and provides indirect evidence for π-anion and π-cation radical formation in the initial electron transfer steps.

Elucidation of the $(Ar_4P)Pt$ oxidation product is of special interest since it was recently demonstrated that an overall two-electron oxidation of $(TPP)Pt^{II}$ gives a stable Pt(IV) porphyrin with the neutral π-ring system, rather than a Pt(II) dication with the doubly oxidized macrocycle.[30] Thus, we wished to determine whether electrochemically initiated conversions between Pt(II) and Pt(IV) porphyrins would occur for other tetraarylporphyrins with different substituents and different oxidation potentials as well as for tetrabenzoporphyrins and tetranaphthoporphyrins having π-extended systems. To answer these questions, it was necessary to obtain UV−visible and ESR

Table 1. Half-Wave Potentials (V vs SCE) for $(Ar_4P)Pt$ in CH_2Cl_2, 0.2 M TBAP (See Chart 1 for Structures)

		oxidation			reduction			
cmpd	$\Sigma\sigma^a$	2nd	1st	$\Delta ox_{(2-1)}$	1st	2nd	$\Delta red_{(1-2)}$	HOMO−LUMO gap (V)[c]
1	−4.20	1.40	0.98	0.42	−1.52			2.50
2	−3.12	1.45	1.03	0.42	−1.50			2.53
3		1.55[b]	1.18	0.37	−1.30	−1.80	0.50	2.48
4	−0.25	1.45	1.15	0.30	−1.30	−1.82	0.52	2.45
5	0.00	1.52	1.20	0.32	−1.30	−1.82	0.52	2.50
6	0.96	1.58[b]	1.20	0.38	−1.30	−1.81	0.51	2.50
7	1.80	1.58[b]	1.30	0.28	−1.16	−1.58	0.42	2.46
8	2.96	1.71	1.40	0.31	−1.14	−1.55	0.41	2.54

[a]Values calculated based on the Hammett substituent constants (ref 35). [b]Irreversible peak potential at a scan rate of 0.10 V/s. [c]As measured electrochemically as the difference between the first reduction and first oxidation potentials.

dx.doi.org/10.1021/ic3003367 | Inorg. Chem. 2012, 51, 6200−6210

Table 2. UV−Visible Spectral Data (λ_{max}, nm, $\varepsilon\times10^{-4}$ M^{-1} cm^{-1}) of Neutral and Doubly Oxidized $(Ar_4P)Pt^{II}$ 1−8 in CH_2Cl_2 Containing 0.2 M TBAP (see Chart 1 for Structures)

	initial Pt(II) porphyrin			doubly oxidized product				
cmpd	λ_{max}, nm (ε)			λ_{max}, nm (ε)			$\varepsilon_{Pt(II)}/\varepsilon_{Pt(IV)}$[a]	assignment[b]
1	404 (29.3)	501(3.1)	541 (1.0)	413 (12.0)	423[s](10.1)	529 (1.4)	1.19	Pt(II) porphyrin dication
2	401 (29.4)	509 (3.0)	540 (1.3)	401 (11.2)	417[s](9.1)	522 (2.6)	1.23	Pt(II) porphyrin dication
3	406 (28.0)	511 (2.4)	541 (0.1)	406[s](6.5)	436[c](7.3)	575[c](0.7)	0.89	Pt(II) and Pt(IV)[d]
4	405 (29.8)	510 (2.2)	542 (0.7)	405[s](10.3)	419 (16.6)	525 (1.5)	0.62	Pt(II) and Pt(IV)[d]
5	401 (26.5)	509 (3.5)	540 (0.7)	405[s](10.5)	418 (21.0)	523 (2.2)	0.50	Pt(IV) porphyrin
6	403 (32.6)	509 (4.0)	539 (1.6)	403[s](9.3)	420 (16.6)	524 (4.9)	0.56	Pt(IV) porphyrin
7	402 (36.2)	510 (3.0)	540 (0.9)	402[s](10.8)	418 (25.9)	526 (2.0)	0.42	Pt(IV) porphyrin
8	403 (37.4)	511 (3.3)	541 (1.2)	403[s](12.2)	418 (36.7)	524 (3.1)	0.33	Pt(IV) porphyrin

[a]Ratio of molar absorptivity for Pt(II) and Pt(IV) species. [b]Prevailing product. [c]Broad peak. [d]Mixture of Pt(II) porphyrin dication and Pt(IV) porphyrin; s = shoulder.

spectroelectrochemical data for these compounds under the same conditions.

The UV−visible and photophysical properties of Pt(II) and Pt(IV) porphyrins have been previously studied.[1,2,11,19,28,38,39] The neutral Ar_4P compounds characterized in this work exhibit typical bands for Pt(II) porphyrin UV−visible spectra, i.e., a sharp Soret band at 401−411 nm and well-defined Q bands at 509−514 and 539−543 nm. Spectral data for the neutral and doubly oxidized compounds **1**−**8** in CH_2Cl_2 containing 0.2 M TBAP are summarized in Table 2, while the spectral data for the singly and doubly reduced porphyrins under the same solution conditions are shown in Table S2, Supporting Information. Examples of the spectral changes, obtained during controlled-potential oxidations of **2** and **7**, are illustrated in Figure 3.

As seen in Chart 1, compounds **2** and **7** differ by the type, number, and positions of substituents in the *meso*-aryl rings. Compound **2** has eight electron-donating *ortho*-OCH_3 substituents with a total Hammett constant, $\Sigma\sigma$, of −3.12, while compound **7** has four electron-withdrawing *para*-CO_2Me substituents with a total $\Sigma\sigma$ value of 1.80. This difference leads to different oxidation potentials for the two compounds, with **7** ($E_{1/2}$ = 1.30 V) being harder to oxidize than **2** ($E_{1/2}$ = 1.03 V) by 270 mV as seen in Table 1.

Despite the difference in oxidation potentials and electron donating/withdrawing properties of substituents on **2** and **7** (see Table 1), the spectra before and after the first controlled potential oxidation of these two compounds are comparable to each other. The Soret and Q bands of the neutral porphyrins both decrease in intensity as the oxidation proceeds, and a new broad band appears in the red-orange region, i.e., at λ_{max} = 613 nm for **2** and at λ_{max} = 600 nm for **7** (see top two spectra in Figure 3). The spectral data suggest that the electron-rich compound **2** and electron-deficient compound **7** both undergo initial oxidation at the macrocycle, which leads to the formation of Pt(II) porphyrin π-cation radicals. This assignment was confirmed by the ESR spectra shown in the inset of Figure 3. A porphyrin π-cation radical is also generated in the first oxidation of the other $(Ar_4P)Pt^{II}$ compounds in the series.

In contrast to the first oxidation (top spectra in Figure 3), the spectral changes during the second oxidation of compounds **2** and **7** are drastically different from each other (middle and lower spectra in Figure 3). In the case of compound **2**, no significant spectral changes occur during the second oxidation, indicating a ring-centered electron abstraction at an applied potential of 1.60 V (Figure 3a, lower graph). However, the second oxidation of compound **7** at 1.70 V shows significant

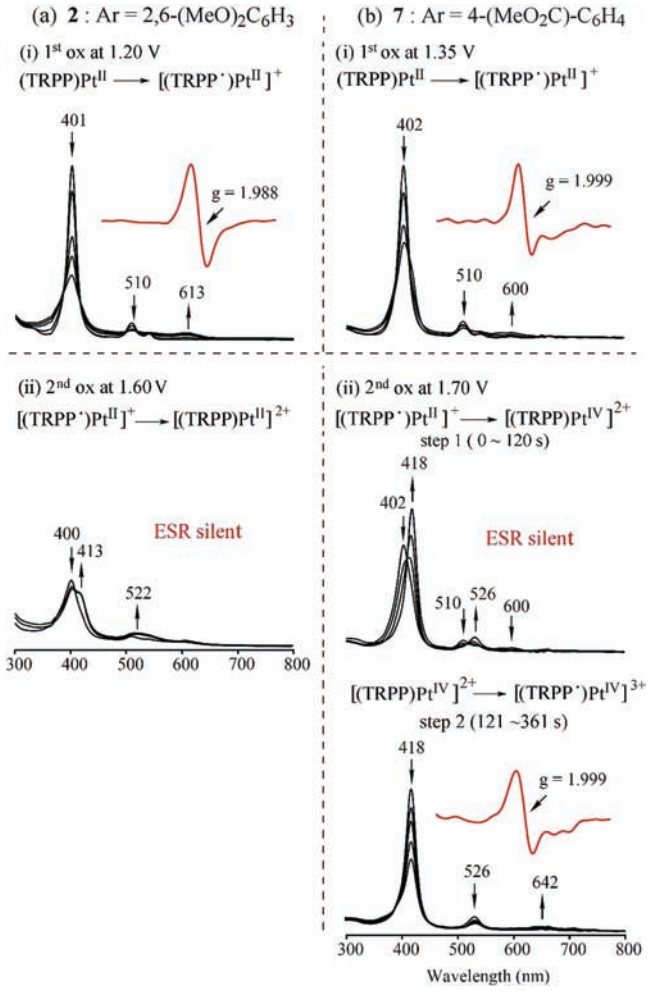

Figure 3. UV−visible spectral changes obtained during controlled-potential oxidation of (a) compound **2** and (b) compound **7** in CH_2Cl_2, 0.2 M TBAP. Insets show ESR spectra of the electrooxidized compounds in the same medium at 77 K.

spectral changes. Two sets of transition were observed as a function of time: the first from 0 to 120 s and the second from 121 to 361 s. In the first two minutes of electrolysis, an intense band appears at 418 nm and a new visible band at 526 nm, both features being characteristic of a Pt(IV) tetraarylporphyrin.[30] This new species is ESR silent, as expected for either a Pt(II) dication or a Pt(IV) porphyrin. Further oxidation of **7** from 121 to 361 s generates an ESR active species, g = 1.999 (lower inset

dx.doi.org/10.1021/ic3003367 | Inorg. Chem. 2012, 51, 6200−6210

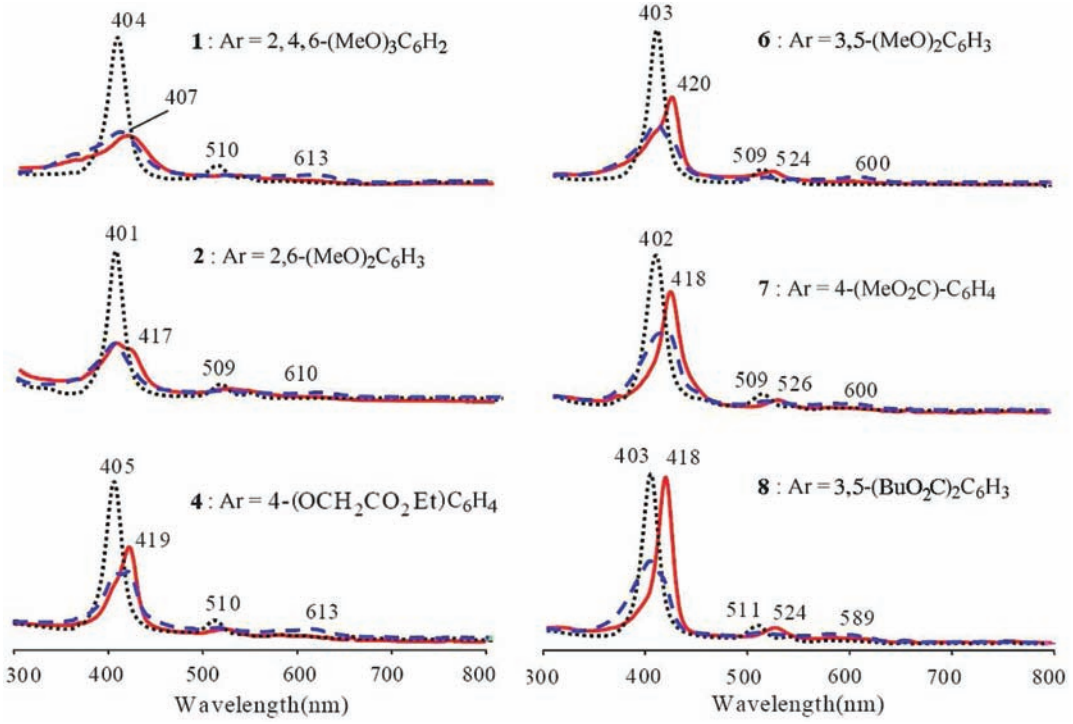

Figure 4. Selected UV–visible spectra of neutral (dotted black line), singly oxidized (dashed blue line), and doubly oxidized (solid red line) Pt(II) tetraarylporphyrins (see Chart 1 for structures) obtained in CH_2Cl_2, 0.2 M TBAP.

of Figure 3b), whose Soret and Q bands at 418 and 526 nm, respectively, have significantly reduced intensity. There is also a new broad band at 642 nm, a feature suggestive of oxidation of the in situ generated Pt(IV) porphyrin with formation of a Pt(IV) porphyrin π-cation radical at the applied potential of 1.70 V. Overall, the two-step spectral changes during the second oxidation of **7** are believed to reflect two sequential one-electron transfer steps, a pattern that has been previously observed during the electrochemically initiated conversion of $(TPP)Pt^{II}$ to $(TPP)Pt^{IV}$.[30]

As will be demonstrated, some of the studied Pt(II) tetraarylporphyrins can be converted to Pt(IV) porphyrins upon oxidation and others cannot, with the ultimate oxidation state assignment of the product being dependent upon the electron-donating or electron-withdrawing nature of substituents on the macrocycle. This can be seen in Table 2 and Figure 4, which illustrate UV–vis spectra of the neutral, singly oxidized, and doubly oxidized tetraarylporphyrins. All six Pt(II) porphyrins shown in Figure 4 (**1**–**2**, **4**, and **6**–**8**) exhibit similar spectral changes between their neutral (dotted black line) and singly oxidized forms (dashed blue line), which suggests the same oxidation mechanism, involving abstraction of one electron from the porphyrin π-ring system. In contrast, UV–visible spectra of the doubly oxidized porphyrins in Figure 4 (solid red line) correspond to two different types of porphyrin products, one with the sharp, well-defined Soret bands at 418–420 nm, and the other with lower and broader Soret bands. An assignment of oxidation state in the doubly oxidized porphyrins is based largely on the known molar absorptivity ratios of the bands in the Soret region for Pt(II) (401–413 nm) and Pt(IV) porphyrins (417–436 nm).[39]

The reduction of compounds **1**–**8** was also monitored in a thin-layer cell. An example of the spectral changes during the process is given in Figure S1, and a summary of the data is listed in Table S2 (see Supporting Information).

The proposed oxidation/reduction mechanism of compounds **1**–**8** is summarized in Scheme 1. The final product

Scheme 1. Proposed Oxidation/Reduction Mechanism of Substituted Pt(II) Tetraarylporphyrins

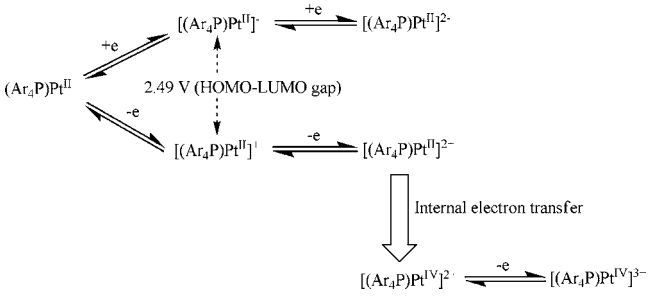

of the first oxidation in all cases is Pt(II) porphyrin π-cation radical, but the product of the second oxidation differs as a function of the macrocycle substituents. Upon abstraction of two electrons, compounds **1**–**2** are converted to relatively stable Pt(II) porphyrin dications, while compounds **5**–**8** form Pt(IV) porphyrins. The in situ generated Pt(IV) porphyrins then can be further oxidized at more positive potentials to give Pt(IV) π-cation radicals, as shown by the ESR data in Figure 3b. Similar M(II) to M(IV) conversions have been reported for lead and palladium octaethylporphyrins.[40] Between the two extremes of electrochemical reactivity, compounds **3** and **4** exist in an equilibrium mixture of a Pt(II) dication and Pt(IV) porphyrin (see Table 2).

Electrochemistry of π-Extended Pt(II) Porphyrins. The potentials for oxidation and reduction of compounds **9**–**14** vary with the type, position, and number of substituents in the macrocycle as well as with the size of the π-extended system. Four of the examined compounds are classified as tetrabenzo-

dx.doi.org/10.1021/ic3003367 | Inorg. Chem. 2012, 51, 6200–6210

Table 3. Half-Wave Potentials (V vs SCE) of (TBP)Pt^{II} and (TNP)Pt^{II} in Different Solvents Containing 0.1 M TBAP

		oxidation			reduction				
solvent	cmpd	3rd	2nd	1st	1st	2nd	3rd	4th	ΔE (V)[c]
CH_2Cl_2	**9**	1.62	1.24	0.76	−1.28	−1.95[a]			2.04
	10	1.75[a]	1.42	0.80	−1.22	−1.58			2.02
	11	1.72[a]	1.22	0.93	−1.00	−1.32	−1.85[a]		1.93
	12	1.80[a]	1.51	1.15	−0.91	−1.17	−1.46	−1.98[a]	2.06
	13		1.13	0.52	−1.25	−1.53			1.77
	14	1.26[a,b]	0.93, 0.80	0.32, 0.13	−1.40	−1.89[a]			1.53
PhCN	**9**	1.60[a]	1.25	0.78	−1.24	−1.89[a]			2.02
	10	1.71	1.36	0.82	−1.16	−1.48	−1.73	−1.92[a]	1.98
	11	1.77[a]	1.05	0.86	−1.05	−1.37	−1.80		1.91
	12	1.81[a]	1.51	1.10	−0.89	−1.19	−1.45	−1.93[a]	1.99
	13		1.01	0.52	−1.19	−1.49	−1.72[a]	−1.85	1.71
	14	1.29[a,b]	0.95, 0.77	0.31, 0.15	−1.42	−1.82			1.57

[a]Peak potential at a scan rate of 0.10 V/s. [b]One more oxidation peak can also be observed at E_{pa} = 1.45 V. [c]The electrochemical HOMO−LUMO gap.

porphyrins (**9**−**12**) and two as tetranaphthoporphyrins (**13** and **14**). The half-wave potentials for these six π-extended porphyrins in CH_2Cl_2 or PhCN containing 0.2 M TBAP are summarized in Table 3, and an example of cyclic voltammograms for two of the porphyrins with fused benzo rings, **9** and **12**, is shown in Figure 5.

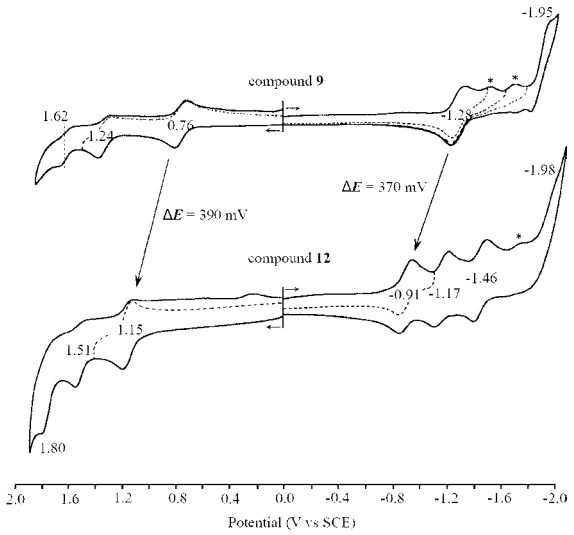

Figure 5. Cyclic voltammograms of **9** and **12** in CH_2Cl_2 containing 0.1 M TBAP. Side products formed from the reduced species are indicated by an asterisk.

The two porphyrins in Figure 5 have identical *meso*-substituents but differ in the number and positions of electron-withdrawing CO_2Me substituents in the fused benzo rings (see Chart 2). The difference in potentials between the first reduction of **9** ($E_{1/2}$ = −1.28 V) and that of **12** ($E_{1/2}$ = −0.91 V) amounts for 370 mV, with **12** being easier to reduce. Almost the same difference in the first oxidation potentials (390 mV) is seen between compounds **9** and **12** (0.76 and 1.15 V), with **12** in this case being harder to oxidize. As expected, the substituent effect of 45 mV per CO_2Me group in the benzo ring is larger than when the same groups are located in the *meso*-aryl rings in the Ar_4P macrocycle. In the latter case, $E_{1/2}$ shifts by 25−35 mV per CO_2Me group (see, for example, the potentials of compounds **5** and **7** in Table 1). Because the substituent effect is almost identical for oxidation and reduction of the two porphyrins in Figure 5, almost the same HOMO−LUMO gap is observed, i.e., 2.04 V for **9** and 2.06 V for **12**.

The solvent also influences redox potentials of π-extended porphyrins. As seen from Figure 6, electroreduction of

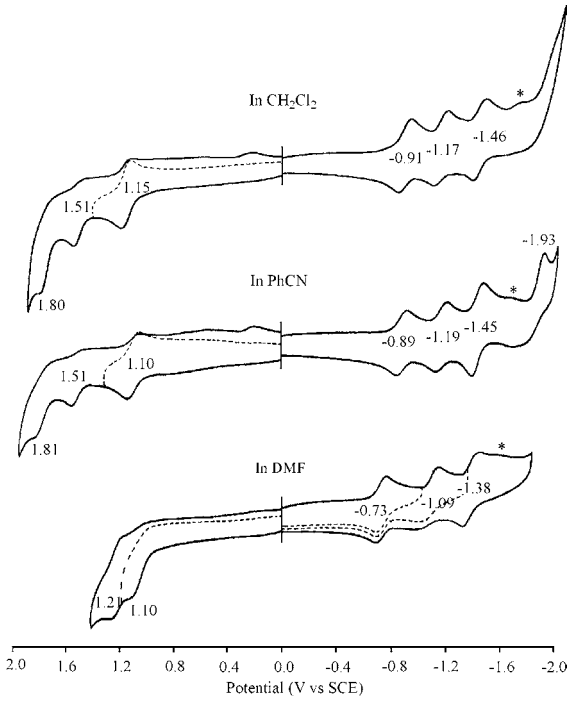

Figure 6. Cyclic voltammograms of compound **12** in CH_2Cl_2 (DN = 0.0), PhCN (DN = 11.9), and DMF (DN = 26.6) containing 0.2 M TBAP. Peaks marked with an asterisk correspond to side products of the reduction.

compound **12** occurs at lower (less negative) potentials with an increase in the donor number (DN) of the solvent, i.e., from 0.0 (CH_2Cl_2) to 11.9 (PhCN) and to 26.6 (DMF).[32,41] Solvents with larger DN and with higher solvation capacity may stabilize anion radicals formed in the Pt(II) porphyrin electroreduction.

A summary of UV−vis spectral data for the neutral, singly oxidized, and singly reduced compounds **9**−**14** in PhCN is given in Table S3, Supporting Information, and examples of the

dx.doi.org/10.1021/ic3003367 | Inorg. Chem. 2012, 51, 6200−6210

spectral changes as a function of applied potential are shown in Figure 7 for (TBP)Pt^{II} **12** in PhCN containing 0.2 M TBAP.

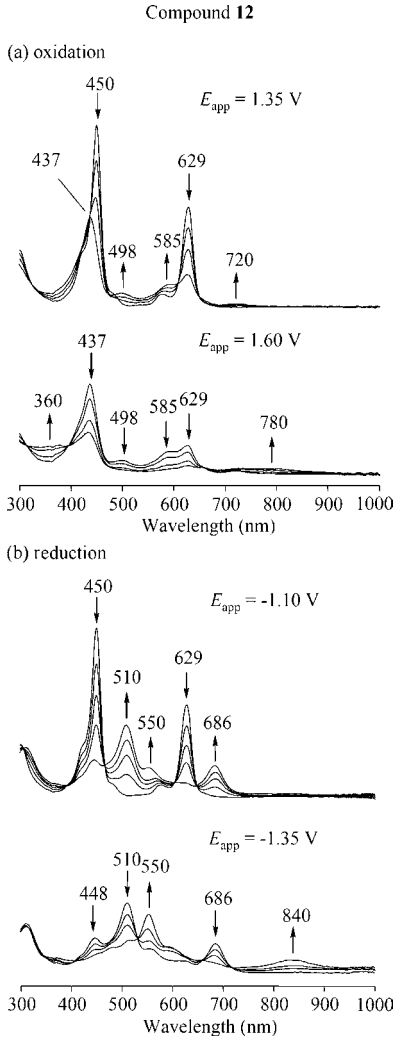

Figure 7. UV−vis spectral changes of compound **12** in PhCN containing 0.2 M TBAP during (a) oxidation and (b) reduction in a thin-layer cell at indicated potentials.

During oxidation at 1.35 V, the Soret and Q bands of the neutral compound decrease in intensity, while a new band of the cation-radical appears near 720 nm (Figure 7a). These changes are consistent with macrocycle-centered electron transfer processes, and the spectrum of the final product is similar to that previously reported for $[ZnTBP]^{+\bullet}$.[42] The Soret and Q bands of the neutral compound **12** also decrease in intensity during the first reduction at an applied potential of −1.10 V, and this change is accompanied by the appearance of three new visible bands at 510, 550, and 686 nm. The final spectrum is assigned to the Pt(II) porphyrin π-anion radical. Spectral changes during the second controlled potential reduction at −1.35 V and the second controlled potential oxidation at 1.60 V are also shown in Figure 7. The spectrum of the doubly reduced form has earlier been assigned to a Pt(II) tetrabenzoporphyrin dianion.[43,44]

Figure 8 shows the dependence of the measured half-wave potentials (in CH_2Cl_2) on the number of fused benzo rings per pyrrolic unit in the macrocycle for compounds **8**, **10**, nd **13**, all of which have identical *meso*-(3,5-$(BuO_2C)_2C_6H_3$) substituents. It can be seen that π-extension result in a large negative shift of $E_{1/2}$ for both oxidations, but the shifts in $E_{1/2}$ for reductions are smaller.

Earlier reports in the literature have analyzed changes in optical spectra upon going from porphyrin to tetrabenzoporphyrin and to tetranaphthoporphyrin.[45−49] Analogous changes in electronic absorption spectra are observed in the present study upon going from a Pt(II) tetraarylporphyrin to the tetrabenzoporphyrin and then to the tetranaphthoporphyrin (Figure 9). When the π-conjugation is increased from $(Ar_4P)Pt^{II}$ (**8**) to (TBP)Pt^{II} (**10**) to (TNP)Pt^{II} (**13**), the lowest energy Q_{00} transitions increase in intensity and decrease in frequency, i.e., λ_{max} of the Q band shifts from 541 nm (**8**) to 620 nm (**10**) to 697 nm (**13**). This result is consistent with what was reported for similar porphyrins with other central metal ions.[48,50]

Narrowing of the HOMO−LUMO gap is apparent in both the spectroscopic and electrochemical data. The absolute potential difference between the first reduction and the first oxidation (the electrochemical HOMO−LUMO gap) changes from 2.46 V for **8** to 2.03 V for **10** to 1.71 V for **13** (in CH_2Cl_2). The spectroscopic values, which represent energies for the $S_0 \rightarrow S_1$ transitions, change as 2.29 eV for **8**, 2.00 eV for **10**, and 1.78 eV for **13**. Because Pt(II) porphyrins are strongly phosphorescent, energies of their lowest triplet electronic states and thus of the $T_1 \rightarrow S_0$ transitions could be determined from their emission spectra. The corresponding values follow the same trend, i.e., 1.87 eV for **8**, 1.57 eV for **10**, and 1.35 eV for **13**, paralleling exactly the $S_0 \rightarrow S_1$ energies with a nearly constant 2*J* value (singlet−triplet splitting energy) of 0.43 eV.

As seen in Table 4, changes in the electrochemical HOMO−LUMO gap induced by annealing of benzo or naphtho groups correlate quite well with spectroscopic energies. However, one should keep in mind that optical transitions of porphyrins cannot be assigned to single excitations, e.g., between the HOMO and LUMO or between the HOMO − 1 and LUMO, etc.;[43] which is due to a strong configuration interaction. Nevertheless, a simplified scheme can be drawn to interpret relationships between the electrochemically measured HOMO−LUMO gap and the energy of an optical transition (Figure S2, Supporting Information).

As seen from the potentials in Table 3, the $E_{1/2}$ values for oxidation of the π-extended Pt(II) porphyrins **9**−**14** occur at much lower potentials than for oxidation of the $(Ar_4P)Pt^{II}$ derivatives **1**−**8** (Table 1). This behavior is consistent with the observed narrowing of the HOMO−LUMO gap due to destabilization of the porphyrin HOMO. Indeed, the a_{1u} HOMO, which resides primarily on the β-pyrrolic carbons in the nonextended macrocycle, experiences destabilization due to an increase in the electronic density, caused by annealing with external aromatic rings. At the same time, small, if any, changes in reduction potentials suggest that the LUMO energies remain practically unaffected by the π-extension. These effects have been demonstrated previously by computations.[46−48]

Finally, we should note that, in the above discussion, we left out nonplanar deformations of the macrocycle and the effect of *meso*-aryl groups, as they influence the redox properties of porphyrins in conjunction with such deformations. These effects, although arguably smaller than the effect of π-extension, are, however, not constant in the series of porphyrins under comparison (compounds **8**, **10**, and **13**). While the metal complexes of Ar_4P have nearly planar structures, Ar_4TBP and Ar_4TNP are known to have highly saddled structures.[19,33,51−53]

dx.doi.org/10.1021/ic3003367 | *Inorg. Chem.* 2012, 51, 6200−6210

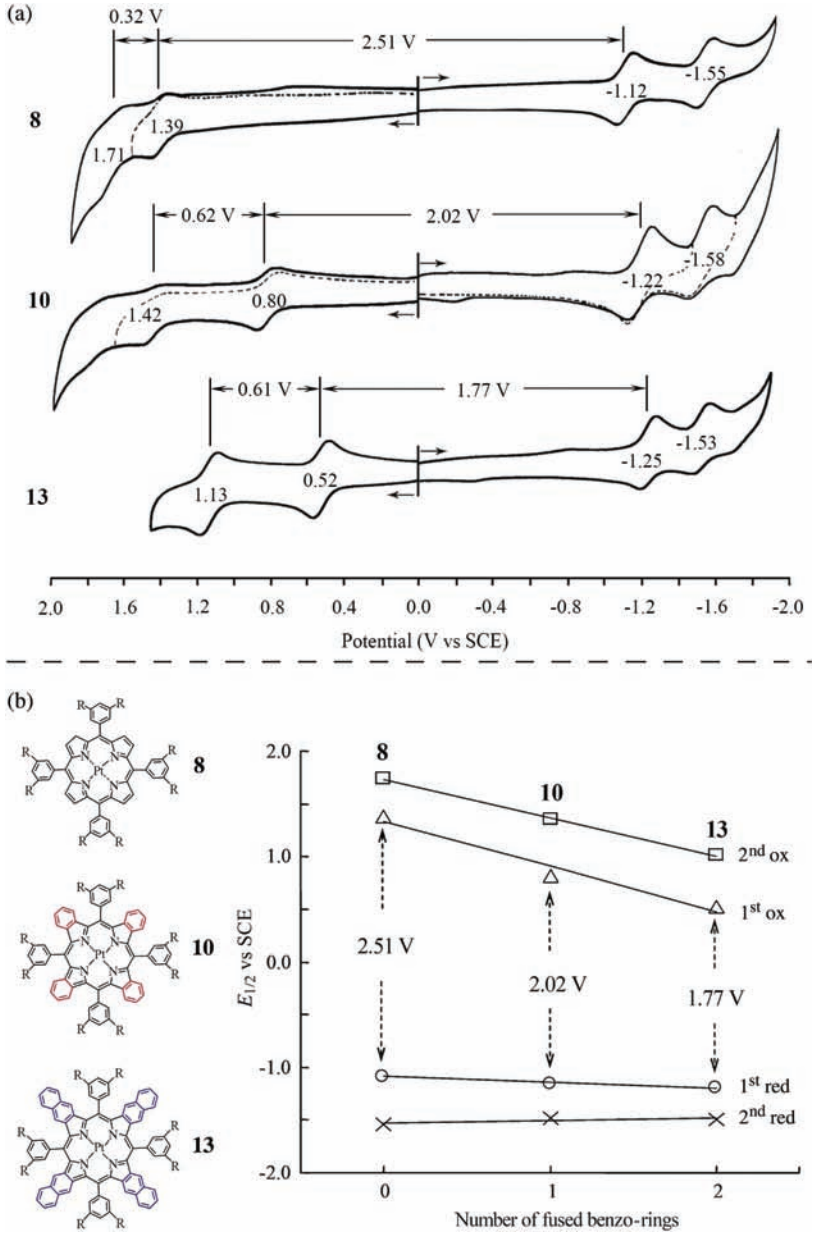

Figure 8. (a) Cyclic voltammograms of compounds **8**, **10**, and **13** in CH_2Cl_2 containing 0.1 M TBAP and (b) changes in half-wave potentials for reductions of compounds **8**, **10**, and **13** with an increase in the number of fused benzo rings (0, 1, or 2 per pyrrolic unit in the macrocycle).

Nonplanarity alone affects the energetics of the porphyrin macrocycle, as known from multiple spectroscopic studies.[54−60] Also, in the case of $(Ar_4P)Pt^{II}$, the *meso*-aryl substituents are oriented at ca. 60° relative to the macrocycle plane;[61] while in nonplanar Ar_4TBP and Ar_4TNP, the effective dihedral angles between the *meso*-aryls and the macrocycle are much smaller. Such smaller angles should facilitate coupling between the corresponding π-systems,[61,62] and the effects of substituents in the *meso*-aryl rings of Ar_4TBP and Ar_4TNP are expected to be larger than in Ar_4P compounds. By looking at the data in Table 4, one can see that the gap between the first oxidation potential of **8** and that of **10** (0.43 V) is larger than the gap between **10** and **13** (0.32 V). This may be due to the fact that, in the former case, both the planarity and the *meso*-aryl coupling significantly change from **8** to **10** in addition to the change in the π-extension. In the second case, going from $(TBP)Pt^{II}$ **10** to $(TNP)Pt^{II}$ **13**, only an increase in the π-extension is present since the degree of nonplanarity remains practically unchanged. An accurate delineation of the effects of nonplanarity and of the *meso*-aryl groups will require a separate study on a special set of model porphyrins.

Interestingly, the oxidation behavior of compound **14** differs from that of compounds **9**−**13** as seen from Figure 10, illustrating cyclic voltammograms for **13** and **14**. The peak currents for the oxidations of compound **14** are only half as large as for the first reduction of the same compound and/or for the oxidations and reductions of **13**. This result suggests that a dimer may form during electrooxidation of **14**. The formation of dimers upon electrooxidations has been observed for cobalt, copper, or nickel complexes of corroles.[63−65] It is worth pointing out that a solvent with large coordination capacity can prevent $\pi-\pi$ stacking and dimer formation. Nevertheless, this appears to not be the case for compound **14**,

dx.doi.org/10.1021/ic3003367 | *Inorg. Chem.* 2012, 51, 6200−6210

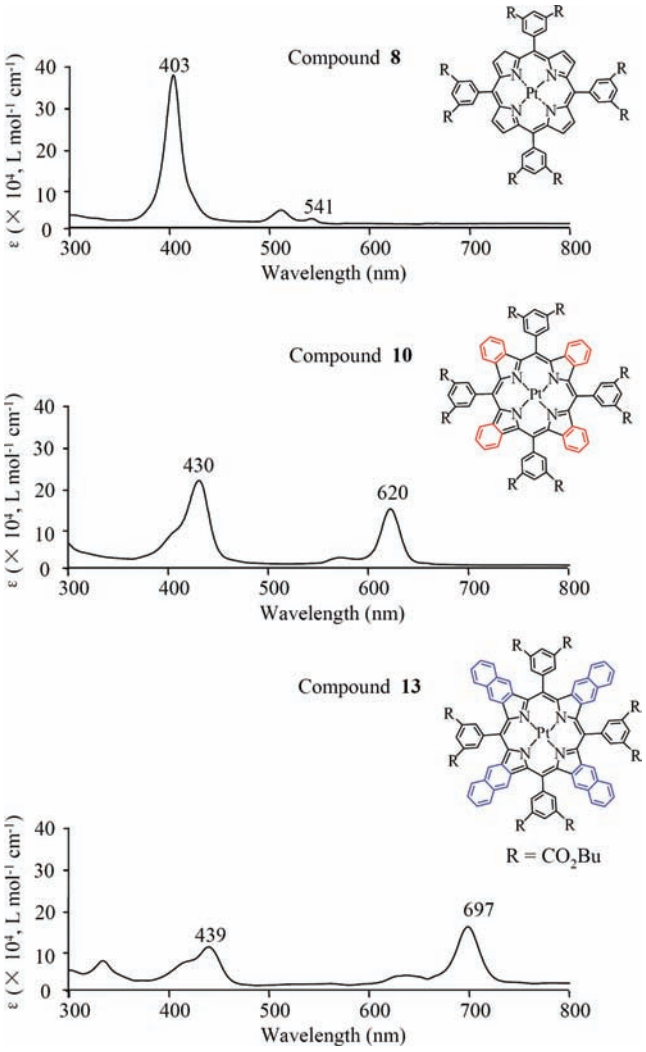

Figure 9. UV−visible spectra in CH_2Cl_2 containing 0.1 M TBAP for compounds **8**, **10**, and **13** having 0, 1, or 2 fused phenyl rings.

Table 4. Changes in Electrochemical HOMO−LUMO Gaps (ΔE) and Lowest Singlet ($E_{S0\rightarrow S1}$) and Triplet ($E_{T1\rightarrow S0}$) Transition Energies for $(Ar_4P)Pt^{II}$ 8, $(TBP)Pt^{II}$ 10, and $(TNP)Pt^{II}$ 13

	$(Ar_4P)Pt^{II} \rightarrow (TBP)Pt^{II}$	$(TBP)Pt^{II} \rightarrow (TNP)Pt^{II}$
$\delta\Delta E$ (V)	−0.43	−0.32
$\delta E_{S0\rightarrow S1}$ (eV)	−0.29	−0.22
$\delta E_{T1\rightarrow S0}$ (eV)	−0.30	−0.22

whose cyclic voltammograms are similar in CH_2Cl_2, PhCN, and DMF (Figure S3, Supporting Information).

CONCLUSIONS

We have reported the electrochemical properties of 14 Pt(II) porphyrins with different electron-donating or electro-withdrawing substituents and different degrees of macrocycle π-extension. In all cases, the first one-electron oxidation and first one-electron reduction are ring-centered and lead to the corresponding π-anion and π-cation radicals. The second reductions result in the formation of Pt(II) porphyrin dianions, but the site of the second oxidation strongly depends on the electronic structure of the macrocycle. For some of the compounds Pt(II) porphyrin dications were electrogenerated, while others were converted to Pt(IV) porphyrins with unoxidized conjugated macrocycles. A correlation was established between the values of oxidation potentials and the degree of the macrocycle π-extension, confirming that a fusion of the macrocycle with external aromatic rings narrows the HOMO−LUMO gap by way of destabilizing the macrocycle-localized HOMO. Understanding these general electrochemical properties of Pt(II) porphyrins is believed to be highly useful in view of their increasing use as components of optical molecular devices with complex energy and electron transfer pathways.[10,66−68]

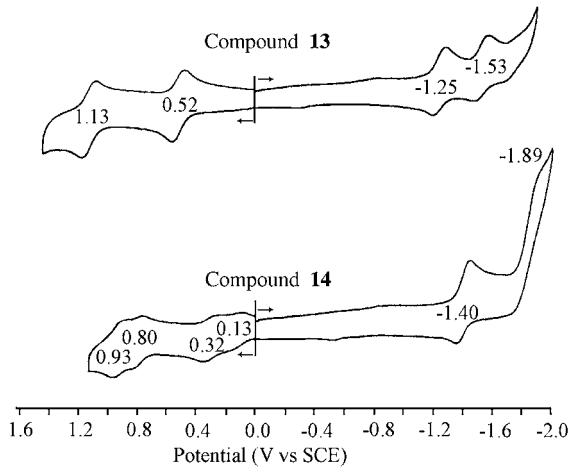

Figure 10. Cyclic voltammograms of compounds **13** and **14** in CH_2Cl_2 containing 0.1 M TBAP.

ASSOCIATED CONTENT

Supporting Information

Half-wave potentials; UV spectal data; effect of π-extension on the HOMO−LUMO gap and excitation energy; cyclic voltammorgram of compound **14**. This material is available free of charge via the Internet at http://pubs.acs.org.

AUTHOR INFORMATION

Corresponding Author

*E-mail: kkadish@uh.edu (K.M.K.); vinograd@mail.med.upenn.edu (S.A.V.); zpou2003@yahoo.com (Z.O.).

Notes

The authors declare no competing financial interest.

ACKNOWLEDGMENTS

Support of the grants E-680 from the Robert A. Welch Foundation (to K.M.K.), 05JDG051 from the Jiangsu University Foundation (to Z.O.), and R01-EB007279 (to S.A.V.) from the US National Institutes of Health are gratefully acknowledged.

REFERENCES

(1) Eastwood, D.; Gouterman, M. *J. Mol. Spectrosc.* **1970**, *35*, 359−375.
(2) Kim, D. H.; Holten, D.; Gouterman, M.; Buchler, J. W. *J. Am. Chem. Soc.* **1984**, *106*, 4015−4017.
(3) Lee, W. W. S.; Wong, K. Y.; Li, X. M.; Leung, Y. B.; Chan, C. S.; Chan, K. S. *J. Mater. Chem.* **1993**, *3*, 1031−1035.
(4) Gouterman, M. *J. Chem. Educ.* **1997**, *74*, 697−702.
(5) Lee, S. K.; Okura, I. *Anal. Sci.* **1997**, *13*, 535−540.

(6) Gillanders, R. N.; Tedford, M. C.; Crilly, P. J.; Bailey, R. T. *Anal. Chim. Acta* **2004**, *502*, 1−6.
(7) Zhang, H. D.; Sun, Y. H.; Ye, K. Q.; Zhang, P.; Wang, Y. *J. Mater. Chem.* **2005**, *15*, 3181−3186.
(8) Brinas, R. P.; Troxler, T.; Hochstrasser, R. M.; Vinogradov, S. A. *J. Am. Chem. Soc.* **2005**, *127*, 11851−11862.
(9) Kose, M. E.; Carroll, B. F.; Schanze, K. S. *Langmuir* **2005**, *21*, 9121−9129.
(10) Finikova, O. S.; Troxler, T.; Senes, A.; DeGrado, W. F.; Hochstrasser, R. M.; Vinogradov, S. A. *J. Phys. Chem. A* **2007**, *111*, 6977−6990.
(11) Borisov, S. M.; Papkovsky, D. B.; Ponomarev, G. V.; DeToma, A. S.; Saf, R.; Klimant, I. *J. Photochem. Photobiol., A* **2009**, *206*, 87−92.
(12) Papkovsky, D. B.; Ovchinnikov, A. N.; Ponomarev, G. V.; Korpela, T. *Anal. Lett.* **1997**, *30*, 699−716.
(13) Koo, Y. E. L.; Cao, Y. F.; Kopelman, R.; Koo, S. M.; Brasuel, M.; Philbert, M. A. *Anal. Chem.* **2004**, *76*, 2498−2505.
(14) Babilas, P.; Liebsch, G.; Schacht, V.; Klimant, I.; Wolfbeis, O. S.; Szeimies, R. M.; Abels, C. *Microcirculation* **2005**, *12*, 477−487.
(15) Papkovsky, D. B.; O'Riordan, T. C. *J. Fluoresc.* **2005**, *15*, 569−584.
(16) Cywinski, P. J.; Moro, A. J.; Stanca, S. E.; Biskup, C.; Mohr, G. J. *Sens. Actuators, B* **2009**, *135*, 472−477.
(17) Fercher, A.; Ponomarev, G. V.; Yashunski, D.; Papkovsky, D. *Anal. Bioanal. Chem.* **2010**, *396*, 1793−1803.
(18) Finikova, O. S.; Lebedev, A. Y.; Aprelev, A.; Troxler, T.; Gao, F.; Garnacho, C.; Muro, S.; Hochstrasser, R. M.; Vinogradov, S. A. *ChemPhysChem* **2008**, *9*, 1673−1679.
(19) Lebedev, A. Y.; Cheprakov, A. V.; Sakadzic, S.; Boas, D. A.; Wilson, D. F.; Vinogradov, S. A. *ACS Appl. Mater. Interfaces* **2009**, *1*, 1292−1304.
(20) Sakadzic, S.; Roussakis, E.; Yaseen, M. A.; Mandeville, E. T.; Srinivasan, V. J.; Arai, K.; Ruvinskaya, S.; Devor, A.; Lo, E. H.; Vinogradov, S. A.; Boas, D. A. *Nat. Methods* **2010**, *7*, 755−U125.
(21) Lecoq, J.; Parpaleix, A.; Roussakis, E.; Ducros, M.; Houssen, Y. G.; Vinogradov, S. A.; Charpak, S. *Nat. Med.* **2011**, *17*, 893−U262.
(22) Gross, E. M.; Armstrong, N. R.; Wightman, R. M. *J. Electrochem. Soc.* **2002**, *149*, E137−E142.
(23) Long, T. R.; Richter, M. M. *Inorg. Chim. Acta* **2005**, *358*, 2141−2145.
(24) Borek, C.; Hanson, K.; Djurovich, P. I.; Thompson, M. E.; Aznavour, K.; Bau, R.; Sun, Y. R.; Forrest, S. R.; Brooks, J.; Michalski, L.; Brown, J. *Angew. Chem., Int. Ed.* **2007**, *46*, 1109−1112.
(25) Sommer, J. R.; Farley, R. T.; Graham, K. R.; Yang, Y. X.; Reynolds, J. R.; Xue, J. G.; Schanze, K. S. *ACS Appl. Mater. Interfaces* **2009**, *1*, 274−278.
(26) Sun, Y.; Borek, C.; Hanson, K.; Djurovich, P. I.; Thompson, M. E.; Brooks, J.; Brown, J. J.; Forrest, S. R. *Appl. Phys. Lett.* **2007**, *90*, 213503.
(27) Graham, K. R.; Yang, Y. X.; Sommer, J. R.; Shelton, A. H.; Schanze, K. S.; Xue, J. G.; Reynolds, J. R. *Chem. Mater.* **2011**, *23*, 5305−5312.
(28) Sommer, J. R.; Shelton, A. H.; Parthasarathy, A.; Ghiviriga, I.; Reynolds, J. R.; Schanze, K. S. *Chem. Mater.* **2011**, *23*, 5296−5304.
(29) Finikova, O. S.; Chen, P.; Ou, Z.; Kadish, K. M.; Vinogradov, S. A. *J. Photochem. Photobiol., A* **2008**, *198*, 75−84.
(30) Ou, Z.; Chen, P.; Kadish, K. M. *Dalton Trans.* **2010**, *39*, 11272−11276.
(31) Kadish, K. M.; Van Caemelbecke, E.; Royal, G. In *The Porphyrin Handbook: Electron Transfer*; Kadish, K. M., Smith, K. M., Guilard, R., Eds.; Academic Press: San Diego, CA, 2000; Vol. *8*, pp 1−97.
(32) Kadish, K. M. *Prog. Inorg. Chem.* **1986**, *34*, 435−605.
(33) Finikova, O. S.; Aleshchenkov, S. E.; Brinas, R. P.; Cheprakov, A. V.; Carroll, P. J.; Vinogradov, S. A. *J. Org. Chem.* **2005**, *70*, 4617−4628.
(34) Finikova, O. S.; Cheprakov, A. V.; Vinogradov, S. A. *J. Org. Chem.* **2005**, *70*, 9562−9572.
(35) Zuman, P. *Substituent Effects in Organic Polarography*; Plenum Press: New York, 1967.
(36) Kadish, K. M.; Morrison, M. M.; Constant, L. A.; Dickens, L.; Davis, D. D. *J. Am. Chem. Soc.* **1976**, *98*, 8387−8390.
(37) Takeda, J.; Sato, M. *Chem. Lett.* **1995**, 939−940.
(38) Callis, J. B.; Gouterman, M.; Jones, Y. M.; Henderson, B. H. *J. Mol. Spectrosc.* **1971**, *39*, 410−420.
(39) Mink, L. M.; Neitzel, M. L.; Bellomy, L. M.; Falvo, R. E.; Boggess, R. K.; Trainum, B. T.; Yeaman, P. *Polyhedron* **1997**, *16*, 2809−2817.
(40) Dolphin, D.; Felton, R. H. *Acc. Chem. Res.* **1974**, *7*, 26−32.
(41) Gutmann, V. *Coord. Chem. Rev.* **1976**, *18*, 225−250.
(42) Vogler, A.; Rethwisch, B.; Kunkely, H.; Huttermann, J.; Besenhard, J. O. *Angew. Chem., Int. Ed.* **1978**, *17*, 951−952.
(43) Gouterman, M. *J. Mol. Spectrosc.* **1961**, *6*, 138−163.
(44) Perrin, M. H.; Gouterman, M.; Perrin, C. L. *J. Chem. Phys.* **1969**, *50*, 4137−4150.
(45) Aartsma, T. J.; Gouterman, M.; Jochum, C.; Kwiram, A. L.; Pepich, B. V.; Williams, L. D. *J. Am. Chem. Soc.* **1982**, *104*, 6278−6283.
(46) Kobayashi, N.; Konami, H. *J. Porphyrins Phthalocyanines* **2001**, *5*, 233−255.
(47) Nguyen, K. A.; Pachter, R. *J. Chem. Phys.* **2001**, *114*, 10757−10767.
(48) Rogers, J. E.; Nguyen, K. A.; Hufnagle, D. C.; McLean, D. G.; Su, W. J.; Gossett, K. M.; Burke, A. R.; Vinogradov, S. A.; Pachter, R.; Fleitz, P. A. *J. Phys. Chem. A* **2003**, *107*, 11331−11339.
(49) Kim, P.; Sung, J.; Uoyama, H.; Okujima, T.; Uno, H.; Kim, D. *J. Phys. Chem. B* **2011**, *115*, 3784−3792.
(50) Rozhkov, V. V.; Khajehpour, M.; Vinogradov, S. A. *Inorg. Chem.* **2003**, *42*, 4253−4255.
(51) Cheng, R. J.; Chen, Y. R.; Wang, S. L.; Cheng, C. Y. *Polyhedron* **1993**, *12*, 1353−1360.
(52) Finikova, O. S.; Cheprakov, A. V.; Beletskaya, I. P.; Carroll, P. J.; Vinogradov, S. A. *J. Org. Chem.* **2004**, *69*, 522−535.
(53) Kadish, K. M.; Finikova, O. S.; Espinosa, E.; Gros, C. P.; De Stefano, G.; Cheprakov, A. V.; Beletskaya, I. P.; Guilard, R. *J. Porphyrins Phthalocyanines* **2004**, *8*, 1062−1066.
(54) Gentemann, S.; Medforth, C. J.; Forsyth, T. P.; Nurco, D. J.; Smith, K. M.; Fajer, J.; Holten, D. *J. Am. Chem. Soc.* **1994**, *116*, 7363−7368.
(55) Ravikanth, M.; Reddy, D.; Chandrashekar, T. K. *Chem. Phys. Lett.* **1994**, *222*, 563−570.
(56) Drain, C. M.; Kirmaier, C.; Medforth, C. J.; Nurco, J.; Smith, K. M.; Holten, D. *J. Phys. Chem.* **1996**, *100*, 11984−11993.
(57) Maiti, N. C.; Ravikanth, M. *J. Chem. Soc., Faraday Trans.* **1996**, *0092*, 1095−1100.
(58) Finikova, O. S.; Cheprakov, A. V.; Carroll, P. J.; Dalosto, S.; Vinogradov, S. A. *Inorg. Chem.* **2002**, *41*, 6944−6946.
(59) Haddad, R. E.; Gazeau, S.; Pecaut, J.; Marchon, J. C.; Medforth, C. J.; Shelnutt, J. A. *J. Am. Chem. Soc.* **2003**, *125*, 1253−1268.
(60) Knyukshto, V. N.; Shul'ga, A. M.; Sagun, E. I.; Zen'kevich, E. I. *Opt. Spectrosc.* **2006**, *100*, 590−601.
(61) Rosa, A.; Ricciardi, G.; Baerends, E. J. *J. Phys. Chem. A* **2006**, *110*, 5180−5190.
(62) Rosa, A.; Ricciardi, G.; Baerends, E. J.; Romeo, A.; Scolaro, L. M. *J. Phys. Chem. A* **2003**, *107*, 11468−11482.
(63) Kadish, K. M.; Adamian, V. A.; Van Caemelbecke, E.; Gueletii, E.; Will, S.; Erben, C.; Vogel, E. *J. Am. Chem. Soc.* **1998**, *120*, 11986−11993.
(64) Guilard, R.; Gros, C. P.; Bolze, F.; Jerome, F.; Ou, Z.; Shao, J.; Fischer, J.; Weiss, R.; Kadish, K. M. *Inorg. Chem.* **2001**, *40*, 4845−4855.
(65) Kadish, K. M.; Shao, J.; Ou, Z.; Gros, C. P.; Bolze, F.; Barbe, J.-M.; Guilard, R. *Inorg. Chem.* **2003**, *42*, 4062−4070.
(66) Whited, M. T.; Djurovich, P. I.; Roberts, S. T.; Durrell, A. C.; Schlenker, C. W.; Bradforth, S. E.; Thompson, M. E. *J. Am. Chem. Soc.* **2011**, *133*, 88−96.
(67) Lebedev, A. Y.; Troxler, T.; Vinogradov, S. A. *J. Porphyrins Phthalocyanines* **2008**, *12*, 1261−1269.
(68) Mani, T.; Niedzwiedzki, D. M.; Vinogradov, S. A. *J. Phys. Chem. A* **2012**, *116*, 3598−3610.